On the Crystallinity Effect on the Gas Sorption in Semicrystalline Linear Low Density Polyethylene (LLDPE)

VICENTE COMPAÑ,[1] L. F. DEL CASTILLO,[2] S. I. HERNÁNDEZ,[2] M. MAR LÓPEZ-GONZÁLEZ,[3] EVARISTO RIANDE[3]

[1]Departamento de Termodinámica Aplicada, ETSII, Universidad Politécnica de Valencia, Campus de Vera s/n. 46022-Valencia, Spain

[2]Departamento de Polímeros, Instituto de Investigaciones en Materiales, Universidad Nacional Autónoma de México, Ciudad Universitaria, Apartado Postal 70-360, Coyoacán, México DF, 04510, Mexico

[3]Instituto de Ciencia y Tecnología de Polímeros (CSIC), 28006 Madrid, Spain

Received 28 March 2006; revised 1 March 2007; accepted 18 April 2007
DOI: 10.1002/polb.21228
Published online in Wiley InterScience (www.interscience.wiley.com).

ABSTRACT: This article describes the solubility of carbon dioxide, ethylene and propane in 1-octene based polyethylene of 0.94, 0.92, 0.904, and 0.87 densities. The isotherms obtained in the gas sorption experimental device display a sorption behavior similar to that of glassy polymers. We apply the dual model to semicrystalline polymers assuming that Henry's sites are related to the amorphous phase, which decreases when the crystallinity percentage increases, whereas the surface of the crystalline phase acts as a Langmuir site with higher gas-polymer affinity than glassy polymers. The good concordance of the calculated k_D values, using the Flory-Huggins theory of polymer diluent mixtures, with the experimental results suggest that Henry's gas sorption fulfills this theory and, therefore, it may be a suitable way to estimate polymer-gas enthalpic interactions. Particularly, the variation of k_D with the crystallinity fraction is exponential and the proportionality of the total sorption with the amorphous content seems only apparent. © 2007 Wiley Periodicals, Inc. J Polym Sci Part B: Polym Phys 45: 1798–1807, 2007

Keywords: gas diffusion; permeability; solubility; sorption

INTRODUCTION

The diffusion or transport of a chemical species of low molecular weight in both rubbery and glassy polymers is a topic of interest in many science and technology fields. Their importance has been growing over the past few years regarding the development of polymer films as separation barriers used for packaging food and beverages, protective cable coatings, encapsulating drugs with controlled delivery, development of contact lenses or manufacturing ion-exchange membranes.[1]

One of the most promising application of polymers comes in the separation of gas mixtures industry, such as helium from natural gas, oxygen from nitrogen, hydrogen, and methane purification.[2,3] Most membranes used in the separation of gas mixtures are made from polymeric substances, with high glass transition temperatures such as polysulfones, polyamides or cellulose triacetate.

The development of new gas separation membranes is oriented to obtain a good balance of two properties, namely permeability and perm-

Correspondence to: V. Compañ (E-mail: vicommo@ter.upv.es)

Journal of Polymer Science: Part B: Polymer Physics, Vol. 45, 1798–1807 (2007)

selectivity. To improve these properties, a better knowledge of the interaction among chemical structure, thermodynamics, and transport parameters is needed.[4–8]

Along these lines, the study of films made from linear PE of low density (LLDPE) and relatively low crystalline degree, has been reported.[9] The interest is the relation between the mechanical analysis and permeation measurements. Thanks to the LLDPE manufacturing characteristics, its flexibility and high elongation modulus, this material was selected to be used for packaging and storing food. Therefore, the study of gas diffusion properties is of great interest, particularly the characterization of CO_2, C_2H_4, and C_3H_8, which is the goal of this article.

Preceding studies using this kind of semicrystalline polyethylene were focused on the role played by the interface effect between amorphous and crystalline boundary, which decreases the diffusion coefficient.[10] Therefore, the assumption of a modified free volume with an impermeable-crystalline component in the material, can help to explain the variation of the solubility coefficient,[11,12] and the changes on permeability P and diffusion coefficient D, with temperature and pressure.

In the present article, we proceed to show that using the modified dual-mode sorption model it is possible to explain the variation of the gas solubility for CO_2, C_2H_4, and C_3H_8, using LLDPE as a function of density or crystalline percentage, at 25 and 35 °C. The results for the solubility coefficient, the affinity parameter and the saturation constant for the gases tested, have been interpreted assuming that the amorphous part of the polymer represents a continuous phase in which Henry's sites are homogeneously distributed, and whose volume fraction decreases when the crystalline fraction increases (first mode of sorption). On the other hand, increasing the percentage of crystallinity increases the microcavities or Langmuir sites in which the restricted diffusion takes place (second mode of sorption), so that the gas Langmuir sorption in semicrystalline LLDPE plays a more important role than Henry's sites. Therefore, this dependence with the crystallinity fraction imposes the control rate to the total sorption, as it will be discussed later.

Finally, considering the polymer–gas interaction into Flory-Huggins interaction parameter[13] for each of the gases studied, the Henry's solubility constant at temperature T is obtained.

Theoretical Background

We use the dual-mode sorption model, but considering a glassy and semicrystalline polymer at $T < T_M$. In the sample are present two phases, the amorphous (am) and the crystalline (cr). Each phase fraction fulfills the relation

$$\alpha_{am} + \alpha_{cr} = 1. \tag{1}$$

There are two components in the amorphous phase, gas and polymer. In the crystalline phase there is no gas component, since this phase is considered impermeable to it. The molar volumetric fraction of the gas and polymer components is indicated by ϕ_A and ϕ_P, such that $\phi_A + \phi_P = 1$.

Thus, in a permeation process the variation of the total Gibbs free energy is only given in the amorphous phase. Considering the difference between the chemical potential per mol for the amorphous phase in presence of the gas component, $\mu(T,p,\phi_A)$, and the chemical potential of the polymeric matrix alone, $\mu_0(T,p)$, we have

$$\Delta\mu = \mu(T,p,\phi_A) - \mu_0(T,p). \tag{2}$$

This expression is applicable to pure amorphous phase samples. When a crystalline phase is present, the actual chemical potential changes are given by

$$\Delta\mu_{am} = \alpha_{am}\Delta\mu. \tag{3}$$

Equation 3 expresses that the difference in the chemical potential varies proportionally to the crystallinity percentage. Now, we want to know how Henry's solubility constant (k_D) depends on this quantity. First, let's consider the sorption quantity or the gas concentration per unit volume inside the membrane (C_A), as established according to Henry's law for low concentrations pressures

$$C_A = k_D p_{A,0}, \tag{4}$$

where k_D is Henry's solubility constant and $p_{A,0}$ is the gas pressure at the beginning of the sorption process. C_A can be written according to the ideal gas equation for the diluted solution case,

$$k_D = \frac{C_A}{p_{A,0}} = a\frac{p_{A,T}}{p_{A,0}}. \tag{5}$$

Here $a = \frac{2.24\times10^4}{RT}$ and $p_{A,T}$ is the gas equilibrium pressure at the sorption cell in the station-

ary state. That is the final state, where it is established the mixture polymer–gas inside the membrane where the gas–polymer mixture occurs.

From the first equality for the chemical potential for mixtures we can obtain the pressure ratio.

According to the mixtures theory, the variation of chemical potential for the gas A in a polymer matrix can be written as

$$\frac{p_{A,T}}{p_{A,0}} = \exp\left(\frac{\Delta\mu_{am}}{RT}\right) = \exp\left(\frac{\alpha_{am}\Delta\mu}{RT}\right). \quad (6)$$

Replacing eq. 6 into eq. 5, we obtain

$$k_D = a\ \exp\left(\frac{\alpha_{am}\Delta\mu}{RT}\right). \quad (7)$$

Now, defining the analogous of eq. 7 for the amorphous contribution as

$$(k_D)_{am} = a\ \exp\left(\frac{\Delta\mu}{RT}\right), \quad (8)$$

and from this two last equations, we can find the logarithm relationship for the actual Henry's solubility constant

$$\log k_D = B - M\alpha_{cr}, \quad (9)$$

where

$$B = \log(k_D)_{am}, \quad (10)$$

and

$$M = \frac{\Delta\mu}{RT}. \quad (11)$$

Taking into account the Balta and Rueda[14] reported data, where a linear regression is established between the crystalline fraction, α_{cr}, and the polymer density (ρ in g/cm^3), namely

$$\alpha_{cr} = 6.0474 \cdot \rho - 4.9899, \quad (12)$$

the actual Henry's coefficient is expressed as a density function

$$\log k_D = B' - M' \cdot \rho, \quad (13)$$

where

$$B' = \log(k_D)_{am} + 4.9899M, \quad (14)$$

and

$$M' = 6.0474\frac{\Delta\mu}{RT}. \quad (15)$$

According to eq. 13, the plot of log k_D versus ρ shows a straight line with negative slope.

On the other hand, the result given by eq. 13 is in disagreement with the current assumption of Michaels and Bixler (see refs. 2 and 3), for the low concentrations and low pressure cases, in which Henry's solubility constant is proportional to the amorphous fraction,[15] that is, $k_D = \alpha_{am}\ (k_D)_{am}$. However, their relation is apparent for the general case for the sorption at any pressure, namely, $S = \alpha_{am}S_{am}$. In Results and Discussion we will proceed to verify this result.

Experimental Determination of Sorption Isotherms

The linear low density polyethylene (LLDPE) used in this study was obtained by coextrusion using the same raw materials, but different processing conditions, prepared from copolymer of ethylene-1-octene (Dow Chemical, Tarragona, Spain) with a content of about 8 mol % of the later comonomer. The commercial densities are 0.94, 0.92, 0.904, and 0.87 g/cm^3. The films were prepared by compression molding between two heating plates at 200 °C for 15 min. Then, the films were cooled at room temperature. In this study, the acronyms for the films in decreasing order of crystallinity have been named LLDPE1, LLDPE2, LLDPE3, and LLDPE4, respectively.

Measurements of the absorbed concentration of carbon dioxide, ethylene and propane were performed at 25 and 35 °C, using the experimental device represented in Figure 1. The interval of pressures measured was between 45 and 800 cmHg.

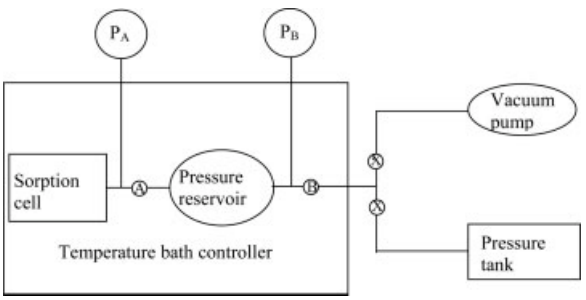

Figure 1. Sorption Experimental cell. A, B, and X are open/close valves.

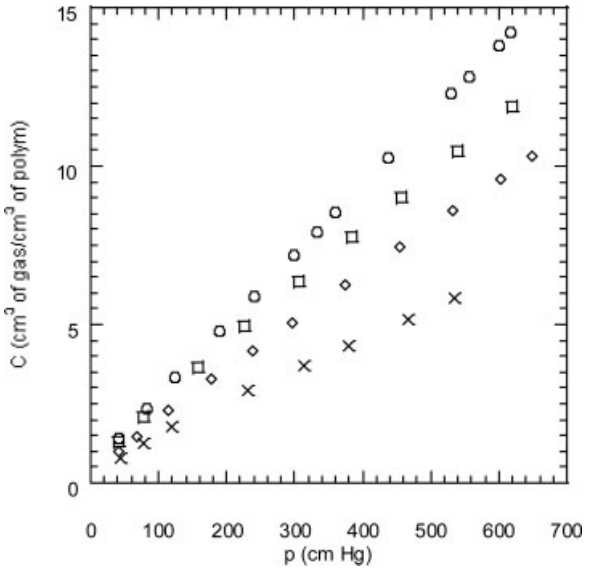

Figure 2. Variation of the concentration of the adsorbed propane for different polyethylens: LLDPE4 (○), LLDPE3 (□), LLDPE2 (◇), and LLDPE1 (×), as a function of the applied pressure at 25 °C.

The polymeric samples were attached in a sorption cell, which was designed to register the number of moles of gas dissolved into the polymeric matrix. P_A gives the pressure in the sorption cell, which is established when valve A is open to allow the gas into the high-pressure reservoir. P_B gives the pressure at the reservoir. Both, the reservoir and the sorption cell are integrated with pressure sensors of range 0–55 bars and 0–11 bars (APR267 and APR266 Pfeiffer model), respectively. The accuracy of the two sensors in each measure was 2%. Each experiment was repeated three times, and the gas concentration sorbed was taken as the average of the values obtained. In all cases differences less than 2% have been obtained. The function of the reservoir is to make sure that the incoming gas from the pressure tank reaches the desired temperature before entering the sorption cell. When thermal equilibrium is obtained, valve B is opened until the pressure P_B is reached and then closed immediately. The gas pressure in the sorption cell diminishes due to the absorption process into the polymeric films, and it is registered each second by an electronic interphase connected to the pressure sensors. Vacuum is made in the sorption cell and pressure reservoir by means of a Leybold AG vacuum pump Trivac D 1,6 B model, which can reach 4×10^{-4} mbar. Before each experiment, the entire system was maintained 24 h under high vacuum. Previous to doing the experiment, the pressure drop and the gas adsorption in the walls were determined.

The expression used to obtain the mole number of the absorbed gas in the films is[16]

$$\Delta n = \frac{V - m/\rho}{RT}\left[\frac{p_i}{z_i} - \frac{p_f}{z_f}\right], \qquad (16)$$

were V is the sorption cell volume, ρ is the polymer density (in g/cm^3) and m is the mass of LLDPE films in the sorption cell (in grams), z_i and z_f represent the compressibility factor of the gas at the initial p_i, and final p_f, pressures, respectively. The values for the compressibility factor were obtained from tables, particularly given in reference,[17] in terms of reduced pressure ($p_r = \frac{p}{p_c}$), and reduced temperature ($T_r = \frac{T}{T_c}$), where p_c and T_c are critical values for pressure and temperature of the adsorbed gas.

The concentration of the adsorbed gas corresponding to the equilibrium pressure $p_{f,}$ given in cm^3 (STp)/(per cm^3 of polymer), is calculated by means of the following relationship:

$$C = \frac{2.24 \times 10^4\ \rho \Delta n}{m}. \qquad (17)$$

RESULTS AND DISCUSSION

Figures 2 and 3, show the variation of the propane and CO_2 concentration versus the pressure for temperatures of 25 and 35 °C, respectively.

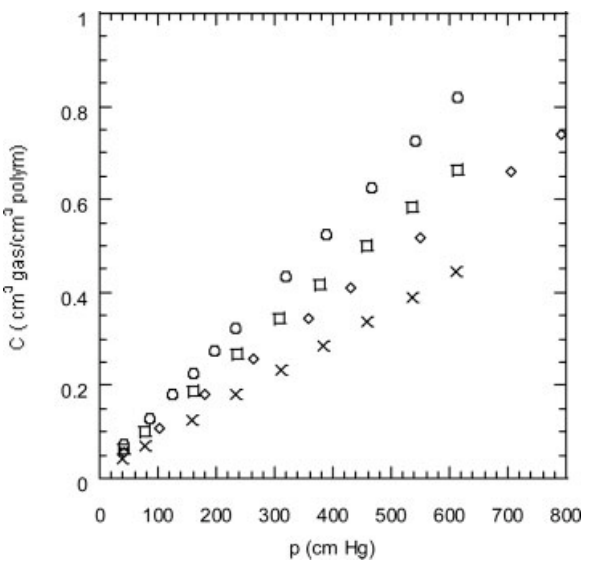

Figure 3. Variation of the concentration of the absorbed CO_2 for different LLDPE as a function of the applied pressure at 35 °C. LLDPE4 (○), LLDPE3 (□), LLDPE2 (◇), and LLDPE1 (×).

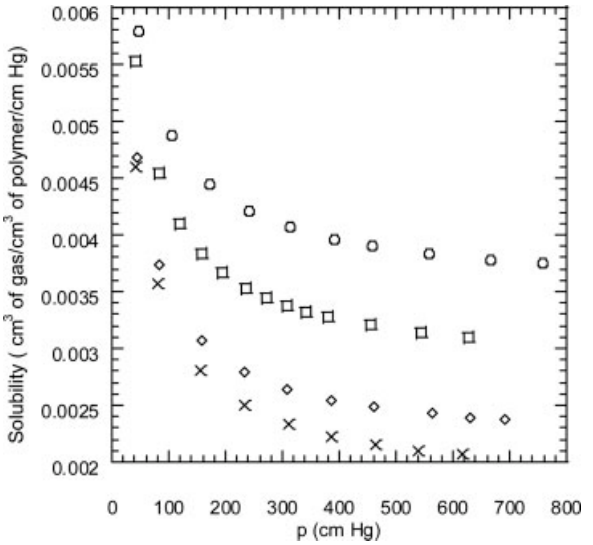

Figure 4. Apparent solubility of ethylene as a pressure function at 25 °C for different LLDPE4 (○), LLDPE3 (□), LLDPE2 (◇), and LLDPE1 (×).

In the previous figures, it can be noted that a drop in pressure occurs near the origin. On the other hand, a linear behavior is observed for pressures higher than atmospheric. This behavior is usually described in glassy polymers by the following equation[18,19]

$$C = k_D \cdot p_{A,0} + \frac{C'_H \cdot b \cdot p_{A,0}}{1 + b \cdot p_{A,0}}. \qquad (18)$$

Similarly, according to the dual-sorption theory, the effective solubility coefficient is expressed by means of two terms: one is the sorption in the amorphous region of the polymer, and the other is that in the microcavities or interphases of crystalline regions (in the case of semicrystalline polymers). Thus it can be expressed by[11]

$$S = k_D + \frac{C'_H \cdot b}{1 + b \cdot p_{A,0}}, \qquad (19)$$

where, C'_H is the Langmuir concentration, b is the polymer–gas affinity parameter and $p_{A,0}$ the applied pressure.

Figures 4 and 5 show the values of the effective solubility of the ethylene and the propane at 25 and 35 °C, respectively, as a pressure function for different polymers with different percentages of crystallinity. It can be noted that the solubility coefficient sharply decreases in the low pressure region, and its value remains nearly constant for $p_{A,0} > 1/b$ values, where the inverse of b represents the characteristic pressure for which deviation of the Henry's law is attained. Since the polymer affinity decreases for semicrystalline polymers, their profile of the sorption curves becomes sharp, taking an "L" form for high crystallinity and temperature. This behavior can be seen in Figure 5.

This behavior can be explained invoking the modified dual-mode, or hereafter, the so-called dual-semicrystalline model.[11,12] It is assumed two different processes of the gas solubility. One is produced in the amorphous part, which decreases as the degree of crystallinity increases. The other is produced into the intercrystalline regions acting as Langmuir sites, and they increase with the crystalline portion.

Nevertheless, when the parameter b and the product $C'_H b$ increase with crystallinity, the resulting profile of the sorption curve is similar to that of amorphous polymers, as it can be seen in Figure 4. Therefore, the interpretation of the dual-semicrystalline model becomes apparent, and the analysis of the variations of the solubility with crystallinity is necessary. This is being done in the time being.

Using a fitting procedure of the experimental data for the effective solubility of the gases tested, it can be noted that the dual-semicrystalline model is fulfilled in the same terms of eq. 19 for our samples. In Figures 4 and 5 the apparent solubility is plotted against the pressure, and they agree with the result of the dual model. The fit parameters are given in Table 1.

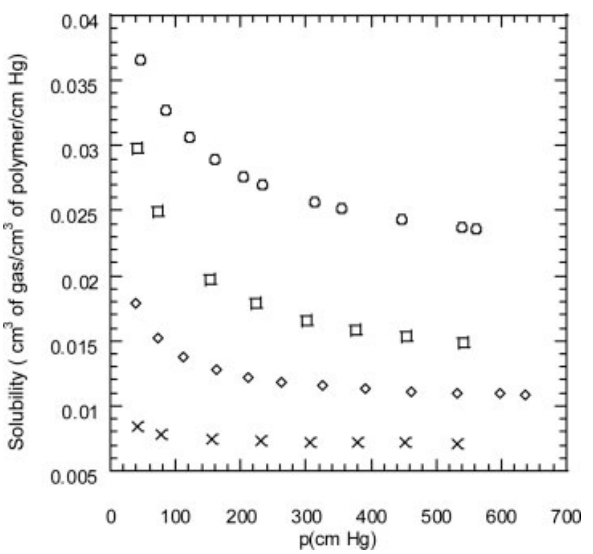

Figure 5. Apparent solubility of propane as a pressure function at 35 °C for LLDPE4 (○), LLDPE3 (□), LLDPE2 (◇), and LLDPE1 (×).

Table 1. Values of the Parameters Related to the First and Second Sorption Modes for CO_2, C_3H_8, and C_2H_4, as a Temperature Function for Several LLDPE with Different Crystallinity

MEMBRANA	Density (g/cm^3)	GAS	T (K)	$k_D \times 10^3$	C'_H b $\times 10^3$	b $\times 10^3$ (cmHg^{-1})
LLDPE1	0.94	CO_2	25	1.10 ± 0.10	0.15 ± 0.02	85 ± 20
LLDPE2	0.92			1.18 ± 0.12	1.15 ± 0.24	70 ± 15
LLDPE3	0.904			1.25 ± 0.13	0.85 ± 0.25	60 ± 14
LLDPE4	0.87			1.40 ± 0.15	0.35 ± 0.10	35 ± 10
LLDPE1	0.94	Ethylene		1.78 ± 0.2	8.2 ± 2.4	45 ± 15
LLDPE2	0.92			2.14 ± 0.2	7.5 ± 1.6	40 ± 16
LLDPE3	0.904			2.50 ± 0.3	6.0 ± 1.2	32 ± 12
LLDPE4	0.87			4.50 ± 0.4	5.1 ± 1.1	25 ± 8
LLDPE1	0.94	Propane		9.15 ± 0.6	12 ± 3	15 ± 5
LLDPE2	0.92			14.7 ± 1.1	18 ± 4	22 ± 8
LLDPE3	0.904			17.5 ± 1.2	28 ± 6	25 ± 7
LLDPE4	0.87			22.2 ± 1.4	52 ± 11	40 ± 15
LLDPE1	0.94	CO_2	35	0.70 ± 0.04	4 ± 2	0.25 ± 0.10
LLDPE2	0.92			0.91 ± 0.06	3 ± 1	0.15 ± 0.05
LLDPE3	0.904			1.05 ± 0.12	2.0 ± 0.5	0.10 ± 0.02
LLDPE4	0.87			1.30 ± 0.16	3.5 ± 0.7	0.20 ± 0.05
LLDPE1	0.94	Ethylene		1.45 ± 0.18	6 ± 2	0.25 ± 0.07
LLDPE2	0.92			1.65 ± 0.16	4.0 ± 1.5	0.20 ± 0.05
LLDPE3	0.904			1.99 ± 0.17	2.0 ± 0.4	0.07 ± 0.02
LLDPE4	0.87			3.4 ± 0.2	1.5 ± 0.5	0.01 ± 0.005
LLDPE1	0.94	Propane		7.0 ± 0.3	10 ± 2	0.15 ± 0.03
LLDPE2	0.92			10.1 ± 0.8	20 ± 5	0.04 ± 0.02
LLDPE3	0.904			14.2 ± 1.1	35 ± 10	0.025 ± 0.01
LLDPE4	0.87			20.4 ± 1.4	25 ± 8	0.012 ± 0.004

The units of k_D are: cm^3 of gas (STp) cm^{-3} of polymer (cmHg)$^{-1}$.
The units of C'_H are: cm^3 of gas (STp) cm^{-3} of polymer.

From the analysis of data in Table 1, we make the following observations. Henry's solubility constant decreases when temperature increases. This is possibly due to the formation of defects near the interface amorphous-crystalline, such that the effective sorption of the Henry's sites decrease.

Furthermore, the values of the C'_H and b for CO_2 are bigger than that obtained in pure polyethylene. This is due to the fact that the attractive interaction between the permeating gas and the polymer in the Langmuir sites increases for CO_2 and ethylene, but decreases for propane.

The value of b seems almost constant, but for the interval of temperatures for each gas, we see that this value increases with the value of the kinetic diameter of the permeating species.

We now proceed to test the prediction of the theoretical approach given in Theoretical Background. For this purpose, the logarithm of the effective solubility coefficient is plotted against the density for the four LLDPE. The results for k_D in Table 1, are presented in Figures 6–8, for the three gases and two different temperatures.

The conclusion of the analysis of Figures 6–8 shows that the prediction presented in eq. 13 is fulfilled. However, this success indicates that the proportionality-rule presented by Michaels and Bixler, that is, $S = \alpha_{am}S_{am}$, is only an approximation, since the contribution of the Henry sites is smaller one order of magnitude than the Langmuir contribution, which in fact, follows this rule. For instance, the proportionality-rule is confirmed in the cases of ethylene and propane in Figures 9 and 10, respectively. It can be seen that the straight lines coincide in $\alpha_{cr} = 1$, which means that the sorption of the crystallinity phase is zero. However, rigorously, this value is different from zero and the extrapolation of the straight lines to this point is only apparent.

Therefore, the dual model for semicrystalline polymers might be modified to include the cases in which the crystalline phase makes contributions to the sorption, as it was pointed out in ref. 20.

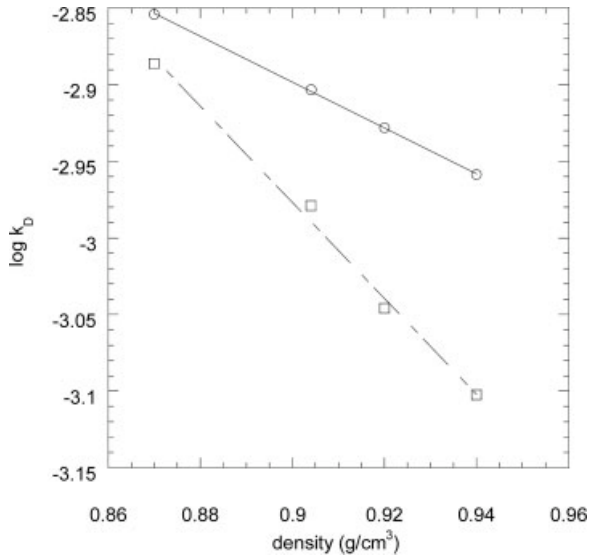

Figure 6. Dependence of the log k_D of CO_2 in LLDPE films with density at 25 (○) and 35 °C (□).

Calculation of Henry's Solubility Constant for LLDPE

According to the Flory-Huggins theory, the variation of chemical potential arising from the mixture of a gas A in the liquid state with a polymer P can be written as[13]

$$\frac{\mu - \mu_0}{RT} = \ln \frac{p_{A,T}}{p_{0A,T}} = \ln \phi_A + \phi_P \left(1 - \frac{\overline{V}_A}{\overline{V}_P}\right) + \chi \phi_P^2. \quad (20)$$

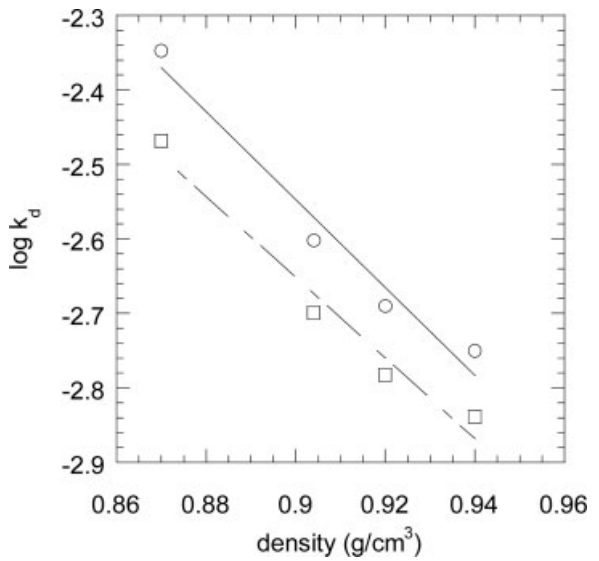

Figure 7. Dependence of the log k_D of ethylene in LLDPE films with density at 25 (○) and 35 °C (□).

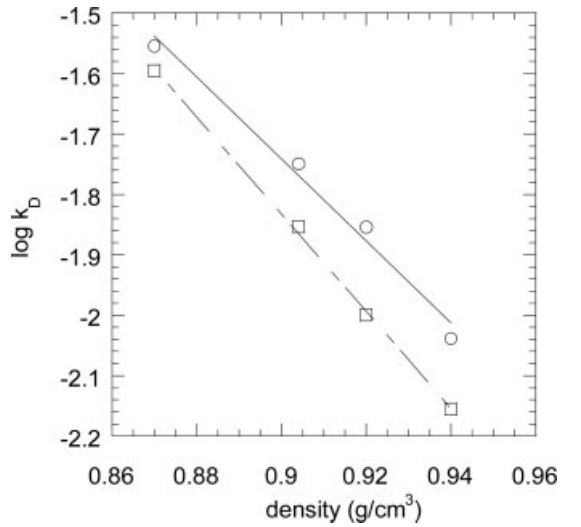

Figure 8. Dependence of the log k_D of propane in LLDPE films with density at 25 (○) and 35 °C (□).

At equilibrium conditions, $p_{A,T}$ represents the vapor pressures of the gas in the liquid state in solution, with the membrane at temperature T. Therefore ϕ_A and ϕ_P are, respectively, the molar volume fractions of gas in liquid form and polymer, so that $\phi_A + \phi_P = 1$.

$\overline{V}_A$ and $\overline{V}_P$ are the respective molar partial volumes, and by taking as reference the boiling point of the gas at 1 atm, the Clapeyron-Clausius

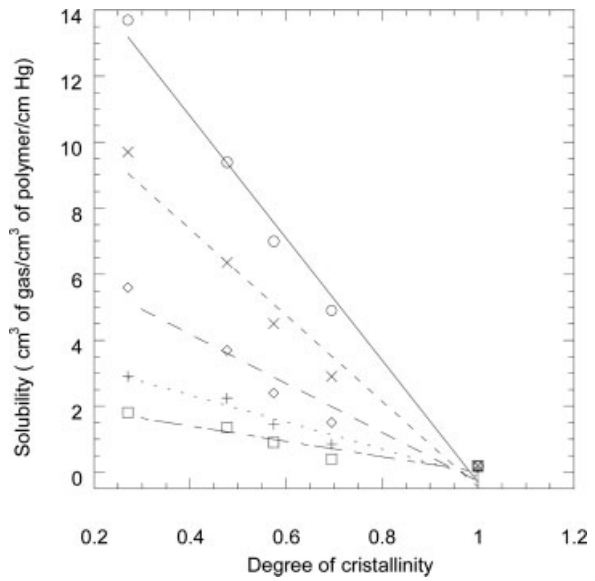

Figure 9. Apparent solubility of ethylene as a pressure function at 35 °C for semicrystalline LLDPE, at differenet pressures: 600 cm of Hg (○), 400 cm of Hg (◇), 200 cm of Hg (×), 100 cm of Hg (+) and 50 cm Hg (□).

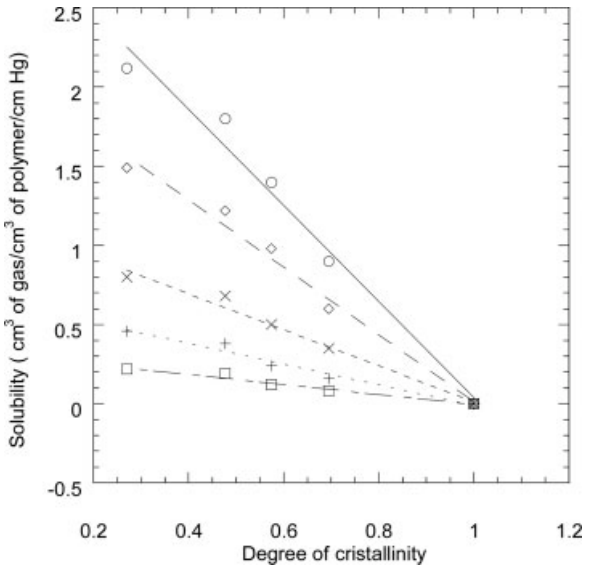

Figure 10. Apparent solubility of propane as a pressure function at 35 °C for semicrystalline LLDPE, at differenet pressures: 600 cm of Hg (○), 400cm of Hg (◇), 200 cm of Hg (×), 100 cm of Hg (+) and 50 cm Hg (□).

equation allows to estimate $p_{A,T}$ as

$$\ln p_{A,T} = \frac{\lambda}{R}\left(\frac{1}{T_{bA}} - \frac{1}{T}\right) = \frac{\lambda}{RT_{bA}}\left(1 - \frac{T_{bA}}{T}\right). \quad (21)$$

Here λ is the latent heat of vaporization and T_{bA} is the boiling temperature of A under 1 atm of pressure. From eqs. 20 and 21 it follows that[8]

$$\ln p_{A,T} = \ln \phi_A + (1 - \phi_A)\left(1 - \frac{\overline{V}_A}{\overline{V}_P}\right) + \chi_A(1 - 2\phi_A + \phi_A^2) + \frac{\lambda}{RT_{bA}}\left(1 - \frac{T_{bA}}{T}\right) \cong \ln \phi_A + (1 + \chi_A) - (1 + 2\chi_A)\phi_A + \frac{\lambda}{RT_{bA}}\left(1 - \frac{T_{bA}}{T}\right). \quad (22)$$

In this expression, the terms with ϕ_A^2, as well as the ratio $\overline{V}_A/\overline{V}_P$, are neglected. It is also considered that $\phi_A \cong \overline{V}_A C_A$, with C_A the molar concentration of gas in the liquid state in the polymeric matrix. Hence, the solubility coefficient can be written as

$$S = \frac{c_A}{p_{A,0}} = (k_D)_{am} \exp(bc_A), \quad (23)$$

where $(k_D)_{am}$ is the Henry's constant at temperature T, given by

$$(k_D)_{amor} = k_D = \frac{22414}{76\overline{V}_A} \exp\left[-(1 + \chi_A) - (\lambda/RT_{bA})(1 - T_{bA}/T)\right]. \quad (24)$$

Here $\overline{V}_A$ and $(k_D)_{amor}$ units are cm^3/mol and cm^3(STP)/(cm^3cmHg), respectively. Equation 24 predicts that the condensability of the gas and/or favorable polymer solvent interactions, enhance greatly the Henry's solubility constant. Moreover, the parameter b in eq. 23 can be written as

$$b = (1 + 2\chi_A)\overline{V}_A. \quad (25)$$

Since $\chi_A \geq 0$ and $T_{bA} < T$, then $S \geq k_D$. On the other hand, at low pressures c_A (0 and the sorption process follows Henry's solubility law. At high pressures, the concentration of gas in the polymer matrix may become significant and, as a result, the isotherms representing the concentration of gas against pressure in rubbery polymers is concave with respect to the ordinates axis. This behavior has experimentally been observed in the sorption isotherms of CO_2 in poly(dimethyl siloxane).[21]

Values of the boiling temperatures under 1 atm of pressure, latent heat of vaporization and the partial molar volume of ethylene, propane, carbon dioxide,[22–24] are shown in Table 2.

We now proceed to obtain the $(k_D)_{am}$ theoretical values, using data in Table 3 in eq. 23, with different values of the interaction parameter. The results are shown in the same Table 3.

Also, the Table 3 shows the results found for Henry's constant using eq. 24, as a function of the interaction parameter. A quick inspection of the data of this table shows that $(k_D)_{amor}$ decreases when the interaction parameter increases. The comparison of these values with those obtained experimentally for CO_2, propane and ethylene, shows that the proper values are

Table 2. Boiling Temperature at 1 atm of Pressure, T_b, Latent Heat of Vaporization, λ, and Partial Molar Volume, $\overline{V}_A$, for Several Gases[22,23]

Gas	T_b (°C)	$10^{-3}\lambda$ (cal/mol)	$\overline{V}_A$ a T_b (cm^3/mol)
CO_2	−78.5	4.112	46
Propane	−42.1	4.487	76
Ethylene	−103.7	3.237	49.3

Table III. The Variation of $(k_D)_{am}$ with the Values of the Interaction Parameters, χ_A at 25 °C for a LLDPE Film with a Specific Density Given by $\rho = 0.94$ g/cm^3

χ_A	$10^3(k_D)_{am}$ CO_2	$10^3(k_D)_{am}$ Propane	$10^3(k_D)_{am}$ Ethylene
0	10.4	158.5	31.1
0.5	6.3	96.1	18.9
1.0	3.8	58.3	11.4
1.5	2.3	35.7	6.9
2.0	1.4	21.5	4.2
2.5	0.8	13.0	2.6
3.0	0.5	7.9	1.5
3.5	0.3	4.8	0.9
4	0.16	2.9	0.6
4.5	0.10	1.8	0.3
5	0.08	1.0	0.2

$\chi_A = 1.7$, 3.5, and 3.0, respectively, considering pure amorphous LLDPE.

CONCLUSIONS

The solubility coefficients of Henry's law and the Langmuir sorption for CO_2, ethylene and propane, were obtained for polymeric films of different densities, varying the temperature, and the applied pressure. From the analysis of these sorption plots the dual model is verified, where it is established that there are two gas sorption modes in a polymeric material. One is around the amorphous nonfreezing sites, which is described by Henry's law, and the other is around the Langmuir sites originated in the freezing regions of the amorphous phase and at the interfaces between amorphous and crystalline boundaries. The crystalline content in the polymer modifies the role played by these sorption modes. The logarithm of Henry's solubility constant varies inversely proportional with the crystallinity percentage. On the other hand, parameters associated to the Langmuir sorption are increasing proportionally to the pure amorphous fraction LLDPE. It should be noted the change in the profile of the sorption curve against pressure, which varies from a hyperbole to an "L" form. That is, the initial part of the sorption curve slows down abruptly (Henry's character diminishes logarithmically), followed by a plateau representing the saturation of the Langmuir sites, which prevails for relatively small pressures.

These two features contribute to establish the dual-semicrystalline model for semicrystalline polymers.[11,12] This might be considered necessary to explain the sorption coefficient changes with temperature and pressure, in polymeric and semicrystalline LLDPE films.

On the other hand, Michaels and Harris J. Bixler's works establish that the total sorption is equal to the product of the amorphous fraction and the solubility constant, for a completely amorphous sample. We concluded, based on the dual-semicrystalline model for semicrystalline polymers, that their results are only an approximation.

This work was supported by the CICYT through Grant No. MAT2005-05,648-C02-02. The authors acknowledge financial support from IMPIVA, de la Generalitat Valenciana through project IMCITA/2005/31. Furthermore, L. F. del Castillo and S. I. Hernández thank to SEP-CONACYT grant 2004-C01-47,070, DGAPA-UNAM Project IN-119606, and they also thank María Teresa Vázquez Mejía and Sara Jiménez Cortés for their help.

REFERENCES AND NOTES

1. Forni, C. Coordinator, quality enhancement and process availability in LLDPE strech film by multisensors and computarized system, Brite- Euram - BE Project 4104; Brussels, 1995.
2. Michaels, A. S.; Bixler, H. J Polym Sci 1961, 50, 393.
3. Michaels, A. S.; Bixler, H. J Polym Sci 1959, 41, 33.
4. Ohya, H.; Kudryavtsev, V. V.; Semenova, S. I. Polyimide Membranes; Gordon and Breach: Tokyo, 1996.
5. Koros, W. J.; Fleming, G. K. J Memb Sci 1993, 83, 1.
6. Stern, S. A. J Memb Sci 1994, 94, 1.
7. Al-Masri, M.; Kricheldorf, H. R.; Fritsch, D. Macromolecules 1999, 32, 7853.
8. Petropoulos, J. H. Pure Appl Chem 1993, 65, 219.
9. Compañ, V.; Ribes, A.; Diaz-Calleja, R.; Riande, E. Polymer 1995, 36, 323.
10. Michaels, A. S.; Parker, R. B., Jr. J Polym Sci 1959, 41, 33.
11. Compañ, V.; López, M. L.; Andrio, A.; Riande, E. Macromolecules 1998, 31, 6984.
12. Compañ, V.; Andrio, A.; López, M. L.; Riande, E. Polymer 1996, 37, 5831.
13. Flory, P. J. Principles of Polymer Chemistry, Cornell University Press: Ithaca, 1953.
14. Balta, C. F. J.; Rueda D. R. Polym J 1974, 6, 216.

15. (a) Tsujita, Y.; Chinese, J. Polym Sci 2000, 18, 301; (b) Membrane Science and Technology; Osada, T.; Nakagawa, T., Eds.; Marcel-Dekker, 1992; pp. 3–58.
16. Koros, W. J.; Paul, D. R.; Rocha, A. A. J Polym Sci: Polym Phys Ed 1976, 14, 687.
17. Hougen, O. A.; Watson, K. M.; Ragatz, R. A. Chem Process Principles, Part II, 2nd ed.; Wiley: New York, 1959.
18. Kesting, R. E.; Fritzsche, A. K. Polymeric Gas Separation Membranes, Wiley-Interscience: New York, NY, 1993.
19. Vieth, W. R.; Sladek, K. J. J Colloid Sci 1965, 20, 1014.
20. Puleo, A. C.; Paul, D. R.; Wong, P. K. Polymer 1989, 30, 1357.
21. Fleming, G. K.; Koros, W. J. Macromolecules 1986, 19, 2285.
22. International Critical Tables of Numerical Date, Physics, Chemistry and Technology; Weshburn, E. W., Ed.; Knovel, 2003, pp. 1926–1930.
23. Kamiya, I.; Naito, Y.; Mizoguchi, K.; Terada, K.; Moreau, J. J Polym Sci Part B: Polym Phys 1997 35, 1049.
24. Reid, R. C.; Prausnitz, J. M.; Poling, B. E. The Properties of Gases and Liquids; McGraw-Hill: New York, 1987.